Protein−Protein Interactions between Cytochrome *b* and the Fe-S Protein Subunits during QH_2 Oxidation and Large-Scale Domain Movement in the bc_1 Complex†

Elisabeth Darrouzet‡ and Fevzi Daldal*

Department of Biology, Plant Science Institute, University of Pennsylvania, Philadelphia, Pennsylvania 19104

Received August 15, 2002; Revised Manuscript Received October 31, 2002

ABSTRACT: The ubihydroquinone:cytochrome (cyt) *c* oxidoreductase, or bc_1 complex, and its homologue the b_6f complex are key components of respiratory and photosynthetic electron transport chains as they contribute to the generation of an electrochemical gradient used by the ATP synthase to produce ATP. The bc_1 complex has two catalytic domains, ubihydroquinone oxidation (Q_o) and ubiquinone reduction (Q_i) sites, that are located on each side of the membrane. The key to the energetic efficiency of this enzyme relies upon the occurrence of a unique electron bifurcation reaction at its Q_o site. Recently, several lines of evidence have converged to establish that in the bc_1 complex the extrinsic domain of the Fe-S subunit that contains a [2Fe2S] metal cluster moves during catalysis to shuttle electrons between the Q_o site and c_1 heme. While this step is required for electron bifurcation, available data also suggest that the movement might be controlled to ensure maximal energetic efficiency [Darrouzet et al. (2000) *Proc. Natl. Acad. Sci. U.S.A. 97,* 4567−4572]. To gain insight into the plausible control mechanism, we used a biochemical genetic approach to define the different regions of the bc_1 complex that might interact with each other. Previously, we found that a mutation located at position L286 of the *ef* loop of *Rhodobacter capsulatus* cyt *b* could alleviate movement impairment resulting from a mutation in the hinge region, linking the [2Fe2S] cluster domain to the membrane anchor of the Fe-S subunit. Here we report that various substitutions at position 288 on the opposite side of the *ef* loop also impair Q_o site catalysis. In particular, we note that while most of the substitutions affect only QH_2 oxidation, yet others like T288S also hinder the rate of the movement of the Fe-S subunit. Thus, position 288 of cyt *b* appears to be important for both the QH_2 oxidation and the movement of the Fe-S subunit. Moreover, we found that, upon substitution of T288 by other amino acids, additional compensatory mutations located at the [2Fe2S] cluster or the hinge domains of the Fe-S subunit, or on the *cd* loop of cyt *b*, arise readily to alleviate these defects. These studies indicate that intimate protein−protein interactions occur between cyt *b* and the Fe-S subunits to sustain fast movement and efficient QH_2 oxidation and highlight the critical dual role the *ef* loop of cyt *b* to fine-tune the docking and movement of the Fe-S subunit during Q_o site catalysis.

The ubihydroquinone:cytochrome (cyt) *c* oxidoreductase, or bc_1 complex,[1] is a key multisubunit membrane component of respiratory and photosynthetic electron transport chains (for reviews see refs *1*−*3*). This enzyme is also homologous to the b_6f complex (plastohydroquinone plastocyanine oxidoreductase) encountered in chloroplasts of higher plants and algae and in cyanobacteria (*4*). The bc_1 complex generates both a pH gradient and a membrane potential ($\Delta\Psi$) via its mechanism of function known as the modified Q cycle (*5*); thus it contributes to the maintenance of a protonmotive force subsequently used by the ATP synthase to produce ATP (*6*). In eukaryotes, the bc_1 complex contains as many as 11 subunits, but in many bacteria it is made up of only 3 catalytic subunits that bear four cofactors: one *c*-type heme on the cyt c_1, two *b*-type hemes (b_L and b_H) on the cyt *b*, and one [2Fe2S] cluster on the Fe-S subunit. The cyt *b* subunit also forms two active sites, for ubihydroquinone (QH_2) oxidation (Q_o) and ubiquinone (Q) reduction (Q_i), located on either side of the cytoplasmic membrane (*3*). A unique electron bifurcation reaction at the Q_o site of the bc_1 complex ensures that one electron of the oxidized QH_2 is conveyed to a high-potential chain constituted by the [2Fe2S] cluster and c_1 heme, while the other electron is transferred to a low-potential chain composed of the b_L and b_H hemes and a Q (or a ubisemiquinone) at the Q_i site. This second branch contributes to the generation of both $\Delta\Psi$ and ΔpH and, hence, is responsible for the energetic efficiency of the enzyme as described by the modified Q cycle mechanism.

† This work was supported by NIH Grant GM 38237 to F.D.

* To whom correspondence should be addressed. Phone: (215) 898-4394. Fax: (215) 898-8780. E-mail: fdaldal@sas.upenn.edu.

‡ Current address: Service de Biochimie Post-génomique et Toxicologie Nucléaire, DIEP, DSV, CEA VALRHO, 30207 Bagnols sur Cèze, France.

[1] Abbreviations: bc_1 complex, ubihydroquinone−cytochrome *c* oxidoreductase; b_H, high-potential *b*-type heme; b_L, low-potential *b*-type heme; cyt, cytochrome; DAD, 2,3,5,6-tetramethyl-1,4-phenylenediamine; E_h, ambient potential; E_{m7}, redox midpoint potential at pH 7; EPR, electron paramagnetic resonance; MOPS, 3-(*N*-morpholino)-propanesulfonic acid; PES, *N*-ethyldibenzopyrazine ethyl sulfate; PMS, *N*-methyldibenzopyrazine methyl sulfate; PMSF, phenylmethanesulfonyl fluoride; Ps, photosynthesis; Q, ubiquinone; QH_2, ubihydroquinone; Q_o, ubihydroquinone oxidation site; Q_i, ubiquinone reduction site; SDS, sodium dodecyl sulfate; SDS−PAGE, sodium dodecyl sulfate−polyacrylamide gel electrophoresis; [2Fe2S], two iron−two sulfur cluster.

10.1021/bi026656h CCC: $25.00
Published on Web 01/24/2003

While the mechanism of the electron bifurcation step at the Q_o site remains unclear, over the years several models have been put forward to rationalize it. These proposals include the "double occupancy" model that attributes two Q/QH_2 molecules at the Q_o site (*7*), the "proton-gated charge transfer" model (*8*), the physical separation of the reactive species with the "rolling over" of a semiquinone species from a [2Fe2S]-proximal to a heme b_L-proximal position (*9*), the formation of a stable intermediate between SQ and the reduced [2Fe2S] cluster until the second electron is transferred to heme b_L (*10*), or the concerted mechanism with a simultaneous interaction of the ubihydroquinone with His161 on the Fe-S subunit and E272 on cyt *b* (*11*). Excitingly, recent crystallographic data have revealed that the [2Fe2S] cluster domain of the Fe-S subunit occupies different positions in various crystal forms (*12*−*15*), suggesting that this domain moves during catalysis. This suggestion has been supported by subsequent crystallographic, spectroscopic, kinetic, and biochemical genetic data (*16*−*25*; see refs *3* and *26* for reviews). This movement is also strongly supported by biochemical and biophysical experiments performed on the homologous complex the b_6f complex (*27*−*29*). Such a device to shuttle electrons between the Q_o site and c_1 heme appears absolutely required for the steady-state turnover of the bc_1 complex as mutants with a nonmoving Fe-S subunit are nonfunctional (*20*−*24*). Moreover, additional considerations also suggest that the movement of the Fe-S subunit needs to be controlled to avoid short-circuiting of the low-potential chain and ensure maximal energetic efficiency (*23*). For example, when Q in the Q_i site is displaced by an inhibitor like antimycin A or the Q_i site is perturbed by a mutation (*30*), the electron residing at the low-potential chain does not come back to reduce the [2Fe2S] cluster, even on a time scale large enough for the Fe-S cluster domain to return back to the Q_o site after delivering its first electron to the c_1 heme. Thus, it appears as if the oxidized [2Fe2S] cluster is somehow inhibited from returning to the Q_o site when no QH_2 is present.

During the catalytic cycle of the bc_1 complex, the movement of the Fe-S subunit might be controlled by conformational changes that occur upon electron or proton transfer events at the Q_o (*31*) or Q_i sites. A next step in the understanding of Q_o site catalysis would be to define the different portions of the bc_1 complex that interact with the Fe-S subunit during its movement. Previously, we had found that a mutation at position L286 of *Rhodobacter capsulatus* cyt *b* could alleviate the movement hindrance resulting from an insertion mutation in the Fe-S hinge region (*23*, *32*). This pointed out possible long-range compensatory interactions between the *ef* loop of cyt *b* and the hinge domain of the Fe-S subunit, two distant domains more than 25 Å apart. In this study, we addressed whether mutations located on other parts of the *ef* loop could also impair the Fe-S subunit movement or the Q_o site catalysis. Examination of known bc_1 complex structures led us to target position 288 of cyt *b* for mutagenesis. Substitution of this position of the *ef* loop with different residues indicated that T288 affects both the movement of the Fe-S subunit and Q_o site catalysis. Furthermore, detailed analyses of the revertants of nonfunctional T288 substitutions revealed that additional second-site mutations at other regions of the bc_1 complex could restore activity. These compensatory mutations were located at either the hinge or the [2Fe2S] cluster domains of the Fe-S subunit or the *cd* loop of cyt *b*. Overall, the findings indicate that the docking of the Fe-S subunit to the Q_o site is spatially adjusted with respect to the *ef* loop of cyt *b* in order to ensure efficient QH_2 oxidation as well as the large-scale domain motion.

MATERIALS AND METHODS

Bacterial Strains and Growth. *Escherichia coli* and *R. capsulatus* strains were grown as described in refs *32* and *33*. Respiratory growth of *R. capsulatus* strains was at 35 °C under semiaerobic conditions in the dark and photosynthetic growth under continuous light and anaerobic conditions. The strain pMTS1/MT-RBC1, considered as the wild-type strain in this study, corresponds to a deletion strain MT-RBC1 (*33*) complemented in trans with the plasmid pMTS1 bearing a wild-type copy of the *petABC* operon encoding the bc_1 complex.

Genetic Techniques. All mutations at position T288 of *R. capsulatus* were introduced by using the QuickChange site-directed mutagenesis kit (Stratagene) with the plasmid pPET1 (a pBR322 derivative bearing a wild-type copy of *petABC*) (*33*) as a template and the following degenerated primers: EDBT288F1 (5′-C CCG CTC TCG BGC CCG GCG CAT ATC GTT CCG) and EDBT288R1 (5′-C GAT ATG CGC CGG GCV CGA GAG CGG GTT GGC) for substituting Thr288 with Gly and Arg residues, EDBT288F2 (5′-C CCG CTC TCG SHC CCG GCG CAT ATC GTT CCG) and EDBT288R2 (5′-C GAT ATG CGC CGG GDS CGA GAG CGG GTT GGC) with Asp, Leu, and Pro residues, EDBT288F3 (5′-C CCG CTC TCG ARS CCG GCG CAT ATC GTT CCG) and EDBT288R3 (5′-C GAT ATG CGC CGG SYT CGA GAG CGG GTT GGC) with Lys, Asn, and Ser residues, and finally EDBT288F4 (5′-C CCG CTC TCG TRC CCG GCG CAT ATC GTT CCG) and EDBT288R1 with Cys and Tyr residues. The 920 bp DNA fragment bearing the generated mutation was cut out of pPET1 with *Xma*I and *Asu*II and exchanged with its counterpart in pMTS1, yielding the plasmid pB:T288X, where X represents the various amino acid residues in the one-letter code. For each mutant, the presence of only the desired mutation on the insert thus exchanged was confirmed by subsequent DNA sequence analysis. These plasmids were then introduced into the bc_1^- strain MT-RBC1 by triparental crosses as described earlier (*33*).

Biochemical and Biophysical Techniques. Chromatophore membranes were prepared in MOPS buffer (50 mM, pH 7.0) containing 100 mM KCl, 1 mM EDTA, and 1 mM PMSF, as described in ref *24*, and protein concentrations were determined according to ref *34*. Sodium dodecyl sulfate−polyacrylamide gel electrophoresis (SDS−PAGE), protein staining, immunoblot analyses, and densitometry scannings were performed as in refs *24* and *25*.

Light-induced, single turnover kinetics for cyt *c* or cyt *b* reduction were performed as described in ref *24* using chromatophore membranes at a concentration of 0.2 μM reaction center (around 0.1 μM bc_1 complex) in the presence of 2.5 μM valinomycin, PMS, PES, DAD, and 2-hydroxy-1,4-naphthoquinone. A single or a double beam monochromator (Biomedical Instrumentation Group, University of Pennsylvania, Philadelphia, PA) was used depending on the

experiments. Transient cyt *c* and cyt *b* reduction kinetics initiated by a short saturating flash (8 μs) from a xenon lamp were followed at 550−540 and 560−570 nm, respectively. With the double beam, the signals corresponding to the two wavelengths were recorded simultaneously and electronically subtracted, and 15 such traces were averaged. With the single beam, 15 traces were recorded and averaged at one wavelength and then at the other wavelength before being mathematically subtracted, and both setups gave very similar traces. The concentrations of antimycin A, myxothiazol, and stigmatellin used were 5, 5, and 1 μM, respectively, and the E_h was poised at 100 mV.

EPR spectroscopy was performed as described in ref *24* on a Bruker ESP-300E at a temperature of 20 K, microwave power of 2 mW, modulation frequency of 100 kHz, and microwave frequency of 9.45 GHz. The chromatophore membrane concentration was about 25 mg of protein/mL (about 4 μM bc_1 complex). Oxidative titrations of the Fe-S subunit [2Fe2S] cluster in chromatophore membranes were conducted potentiometrically according to Dutton (*35*) in the presence of 100 μM tetrachlorohydroquinone, DAD, 1,2-naphthoquinone-4-sulfonate, and 1,2-naphthoquinone. The samples with Q pool oxidized were obtained by incubating them on ice for 10 min with 20 mM ascorbate in the presence or absence of 100 μM stigmatellin.

Chemicals. All chemicals were as described earlier (*36*).

RESULTS

Choice of the T288 Position on the ef Loop of Cyt b. Our previous findings indicated that the hindrance to the movement of the Fe-S subunit resulting from the insertion of an Ala residue in the Fe-S subunit hinge domain (between positions 46 and 47 in *R. capsulatus*) (*23*) could be overcome by a second mutation changing Leu286 to Phe (*32*). This residue lies at the edge of the *ef* loop of cyt *b* on the mitochondrial bc_1 complex structure (*13*, *14*) and is located 6−7 Å away from Thr264 (corresponding to *R. capsulatus* T288). Thr264 is at a distance of less than 3 Å from the amino acid residues His141, Leu142, Cys144, and Ile147 (bovine numbering) in the immediate vicinity of the [2Fe2S] cluster of the Fe-S subunit. Examination of the available structures with Fe-S subunit cluster domain in the c_1, intermediate, stigmatellin, or *b* positions (*13*, *14*; S. Iwata, privileged communication) indicated that the amino acid residue facing Thr264 changes depending on the position of the Fe-S subunit, but a residue always occupies this position. In addition, the Fe-S subunit residues interacting most directly with Thr264 on the *ef* loop are located around the [2Fe2S] cluster and often belong to the conserved box I or box II sequences that provide its ligands. These observations suggested to us that the nature of the amino acid side chain at position 264 of the *ef* loop of cyt *b* (288 in *R. capsulatus*) might play a critical role during Q_o site catalysis.

The Amino Acid T288 Is Critical for the Function of the bc_1 Complex. To probe the role of the *ef* loop of cyt *b*, several substitutions (G, R, D, L, P, K, N, S, C, and Y) were engineered as described in Materials and Methods at position 288 of the *R. capsulatus* cyt *b* subunit or obtained as same-site revertants (T288I and T288V) of the initial mutants (T288S and T288D or T288G, respectively; see below). The effects of these substitutions on the bc_1 complex assembly and function were investigated, and the results obtained are summarized in Table 1. Of the substitutions examined, T288L, T288I, T288V, T288C, and T288G exhibited different degrees of photosynthetic (Ps) growth abilities with the latter two being much slower than a wild-type strain, while T288D, T288K, T288N, T288P, T288R, T288S, and T288Y were all Ps^-. Thus, the nature of the amino acid at this position was critical for Ps growth of *R. capsulatus* and, therefore, for the function of its bc_1 complex. Next, to determine whether in these mutants the absence of the bc_1 complex activity was due to a perturbed assembly or stability of the enzyme, the amounts of the cyt *b*, cyt c_1, and Fe-S subunits and of the [2Fe2S] cluster were determined by SDS−PAGE/immunoblot analyses as described in ref *24* and by EPR spectroscopy, respectively. Usually, to estimate the cluster amounts, the amplitude of the g_y signal of the [2Fe2S] cluster in mutants could be compared to that of a wild-type strain. However, in mutants with perturbed Q_o sites both the shape of the g_x peak and the amplitude of the g_y signals are often altered, which complicates these measurements. To circumvent this difficulty, we used the g_y signals obtained in the presence of the Q_o site inhibitor stigmatellin as all mutants responded properly to this inhibitor. The data indicated that while chromatophore membranes of all mutants exhibited amounts of cyt *b* and cyt *c* subunits per amount of

Table 1: Various Properties of the T288X Substitutions

strain	Ps phenotype[a]	assembly: Fe-S subunit[b]	assembly: [2Fe2S] cluster[c]	EPR g_x[d]	E_{m7} (mV)[e]	electron transfer rate (%)[f]	movement[g]
WT	+	100	100	1.800	310	100	fast
B:T288C	slow	65	13	nd[h]	nd	4	nd
B:T288G	very slow	100	100	1.770	nd	7	fast
B:T288K	−	60	40	1.780	nd	0	fast
B:T288L	+	60	85	1.798	nd	25	fast
B:T288N	−	120	95	1.770	270	3	fast
B:T288S	−	125	120	1.773	255	0	slow
B:T288Y	−	75	50	1.761	nd	0	fast
B:T288I[i]	+	nd	nd	1.806	nd	35	fast
B:T288V[i]	+	90	95	1.806	nd	50	fast

[a] (+) or (−) indicates ability or inability, respectively, to grow photosynthetically in MPYE-enriched medium, and slow or very slow indicates Ps growth at a rate lower than that of a wild-type strain. [b] Fe-S subunit refers to the stoichiometry of the Fe-S subunit to cyt c_1 or cyt *b* subunits as determined by scanning of the SDS−PAGE gels and immunoblots as described in ref *24* and is expressed as a percentage of the wild type. [c] [2Fe-2S] cluster refers to the relative amounts of the [2Fe-2S] cluster in the mutants in comparison with the wild type, as determined by the amplitudes of the EPR g_y signals in the presence of the inhibitor stigmatellin and normalized for protein concentrations used. [d] Position of the g_x resonance in the absence of inhibitor and with the Q_{pool} oxidized. [e] The E_{m7} values were obtained by fitting the EPR g_y signal amplitudes during potentiometric titration of the [2Fe2S] cluster as in ref *24*. [f] Electron transfer rate reflects single turnover bc_1 complex activity and corresponds to the average of QH_2 to cyt *c* and QH_2 to cyt *b* electron transfer rates. These rates expressed as a percentage of that of the wild-type enzyme (approximately 300 and 500 s^{-1} for cyt *c* rereduction and cyt *b* reduction kinetics, respectively) were not significantly different from each other and were determined as described in Materials and Methods. [g] Fast or slow movement is defined as described in ref *23* and depends upon whether the initial phase corresponding to the electron transfer from the [2Fe2S] cluster to c_1 heme in the presence of myxothiazol is visible or not. [h] nd: not done. [i] Mutants T288I or T288V are the same site revertants of T288S or T288D and T288G, respectively. The values shown for T288V are the average of the data obtained with T288I or T288V, which were similar.

total proteins comparable to those found in a wild-type strain, some of them contained substoichiometric amounts of the Fe-S subunit (Table 1). The mutants T288G, T288N, T288V, and T288S exhibited no assembly defect. Others like T288C contained about 65% of the Fe-S subunit with respect to a wild-type strain and barely detectable (13% of the wild type) [2Fe2S] cluster, unless additional precautions, such as addition of 10% glycerol and 20 mM sodium ascorbate (which increased up to 30% the amount of [2Fe2S] cluster), were taken during the chromatophore membrane preparations (Table 1). Nevertheless, the assembly defects seen here were more moderate than those observed previously in the Fe-S subunit hinge deletion mutants (*24*), which still retained their Ps growth abilities. Thus, a defective assembly could not account fully for the lack of the bc_1 complex activity in the T288X mutants examined here.

Most of the T288X Mutants Have Perturbed [2Fe2S]−Q Interactions at the Q_o Site. Further insight into the primary cause of the absence of the bc_1 complex activity in the T288X mutants was sought by analyzing the interactions of the [2Fe2S] clusters with the Q_o site occupants, as it is known that the EPR signature of the reduced [2Fe2S] cluster is very sensitive to its environment (*7*, *37*−*41*). The EPR spectra obtained with several T288X mutants (Figure 1A), in particular the g_x values spreading from 1.780 for T288K to 1.761 for T288Y (Table 1), indicated that the interactions of the [2Fe2S] cluster with Q were perturbed in all cases except the T288L, T288I, and T288V substitutions. However, all substitutions gave rise to a $g_x = 1.785$ signal in the presence of stigmatellin (*38*) (not shown), indicating that the Fe-S subunit responded to this inhibitor as observed previously. In the presence of myxothiazol, the g_x resonance of the [2Fe2S] cluster in the T288L and T288K substitutions became broader with a value of about 1.775 (data not shown). For the remaining mutants, it was impossible to ascertain whether their bc_1 complexes responded properly to myxothiazol as their g_x signals were very broad even in its absence. The T288N and T288S substitutions, which exhibited no assembly defects, were further used to determine the E_m values of their [2Fe2S] clusters. EPR redox titration indicated that both mutants had lower E_{m7} values (255 and 270 mV) in comparison with a wild-type [2Fe2S] cluster (310 mV) (Table 1 and Figure 2). It was noted that, with the Q_{pool} oxidized, the EPR signature of these substitutions resembled more to a native bc_1 complex inhibited by class I inhibitors such as myxothiazol or MOA-stilbene (*40*, *42*).

Most of the T288X Mutants Have Impaired Electron Transfer Rates. Next, the effect of the T288X substitutions on the bc_1 complex activity were analyzed by monitoring light-induced, single turnover cyt *c* rereduction and cyt *b* reduction kinetics, as performed previously (*24*) and also described in ref *43*. In all cases, the data indicated comparable impairments for the QH_2 to cyt *c* and QH_2 to cyt *b* branches, in agreement with a concerted mechanism for QH_2 oxidation at the Q_o site via a bifurcated electron transfer like the one described in ref *11* (Table 1 and Figure 3). Of the mutants analyzed, T288L, T288I, and T288V exhibited sizable electron transfer activities (about 25%, 35%, and 50%, respectively, of a wild-type strain) while the others had very low (less than 5−10% of the wild type) cyt *c* rereduction and cyt *b* reduction rates, in agreement with their defective Ps growth and substoichiometric bc_1 complexes. Thus, with the exception of the hydrophobic substitutions L, I ,and V, the other mutations at position 288 perturbed drastically the catalytic turnover of the enzyme and prevented QH_2 oxidation.

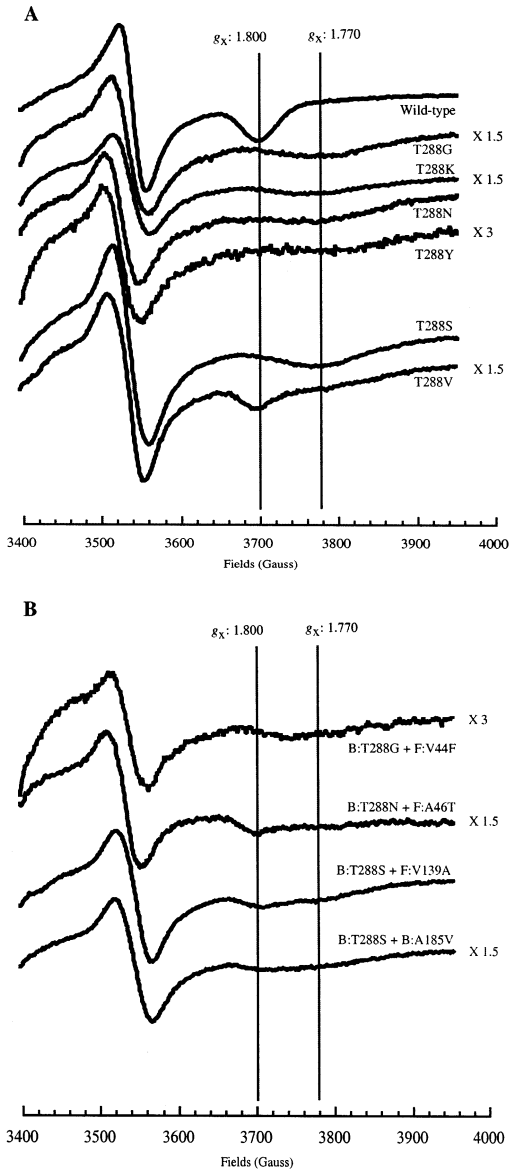

FIGURE 1: EPR spectra of the [2Fe2S] cluster of various T288 mutants and their revertants. The EPR spectra of the wild type and the different T288X mutants were obtained using chromatophore membranes after ascorbate reduction as described in ref *24*. Vertical lines indicate the g_x values of 1.800 and 1.77 as references, and $\times 1.5$ and $\times 3$ refer to the scaling factor used to plot the spectra for various mutants. Panel A shows the spectra for the B:T288G, B:T288K, B:T288N, B:T288Y, B:T288S, and B:T288V substitutions, and panel B shows the spectra for the double mutants B:T288G + F:V44F, B:T288N + F:A46T, B:T288S + F:V139A, and B:T288S + A185V, with B and F referring to the mutations in the cyt *b* and the Fe-S subunits, respectively.

The T288S Substitution Also Interferes with the Movement of the Fe-S Subunit. The effect of the T288X substitutions on the movement of the Fe-S subunit was next probed by monitoring cyt *c* rereduction kinetics (*23*). We have recently demonstrated that the kinetics of electron transfer from an initially reduced [2Fe2S] cluster to c_1 heme, in the presence of myxothiazol, which renders this electron transfer independent of QH_2 oxidation, also encompasses the movement of the Fe-S subunit from the Q_o site to the c_1 position (*23*,

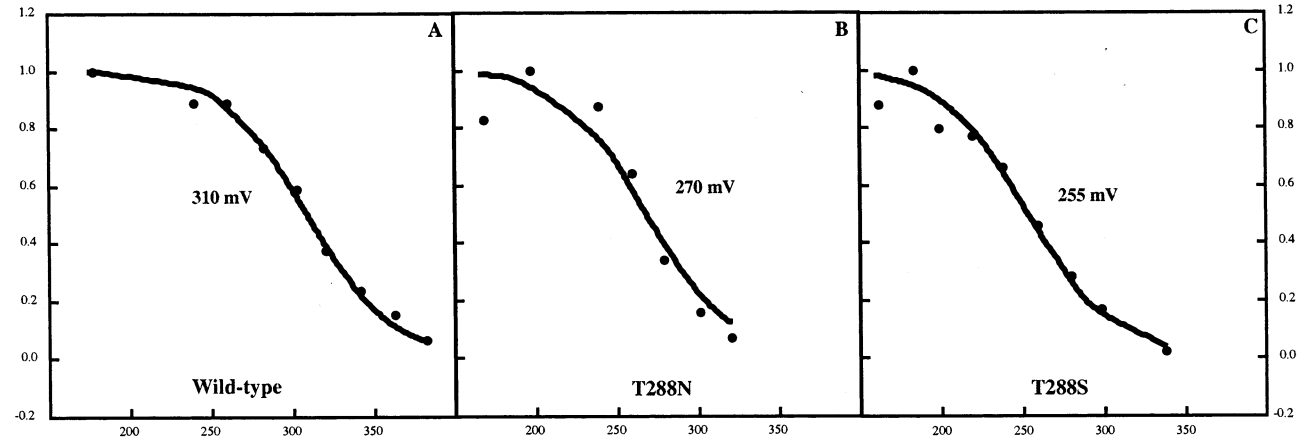

FIGURE 2: Potentiometric dark titrations of the [2Fe2S] cluster of the T288N and T288S mutants. The potentiometric titrations of the [2Fe2S] cluster E_m of the wild-type strain and the B:T288N and B:T288S mutants are shown in panels A, B, and C, respectively. In each case, the amplitude of the EPR g_y signal was recorded between the E_h values of 150 and 350−400 mV, normalized, and fitted to an $n = 1$ Nernst equation to deduce the indicated E_{m7} values, as described previously in ref *24*. The symbols and the line represent the experimental data and the curve fit, respectively.

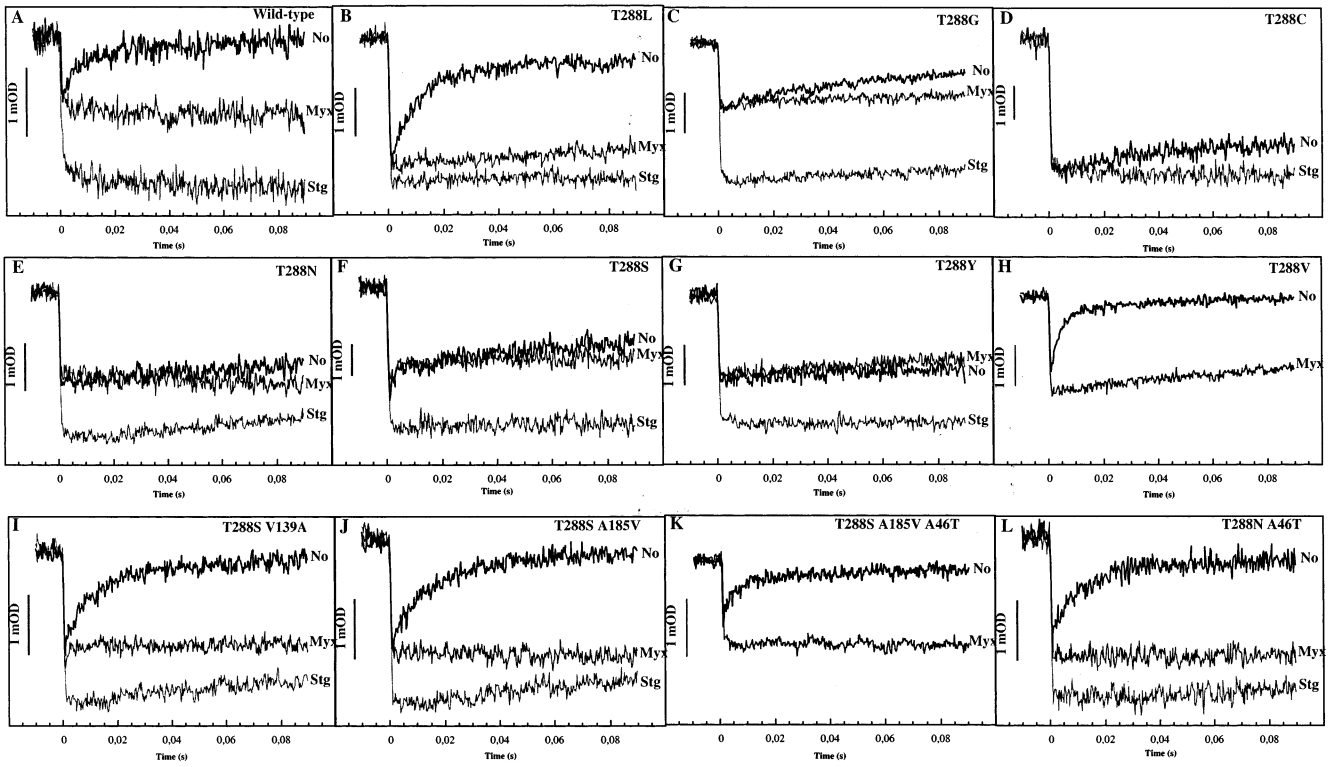

FIGURE 3: Cyt *c* rereduction kinetics in the presence of myxothiazol or stigmatellin in various T288X substitutions and their second-site suppressors. Cyt *c* rereduction kinetics triggered by flash activation of the photochemical reaction center were recorded using chromatophore membranes as described in refs *23* and *24*. In each case, the traces obtained with no inhibitor (no) or in the presence of myxothiazol (Myx), where no QH_2 oxidation takes place at the Q_o site, or in the presence of stigmatellin (Stig), where no electron is transferred from the [2Fe2S] cluster to the c_1 heme are shown. Panels A−L correspond to the wild-type strain, B:T288L, B:T288G, B:T288C, B:T288N, B:T288S, B:T288Y, B:T288V, B:T288S + F:V139A, B:T288S + B:A185V, B:T288S + B:A185V + F:A46T, and B:T288N + F:A46T substitutions, respectively, where B and F refer to the cyt *b* and Fe-S subunits, respectively. For T288V and for the triple mutant B:T288S + B:A185V + F:A46T, the traces in the presence of stigmatellin have not been recorded.

24). In the native enzyme, or in the Q_o site deficient mutants such as Y147A (*44*), this electron transfer step is too fast to be time resolved at a millisecond time scale. However, if the movement of the Fe-S subunit slows down as in the +1Ala mutant (insertion of one Ala residue between positions 46 and 47 of the Fe-S subunit) or the 3ProΔ3 mutant (equivalent to a deletion of amino acid residues 44−49 of the Fe-S subunit and insertion of three Pro residues instead), then it becomes visible (*23*, *24*). When the T288X substitutions were analyzed in this manner, in all cases except T288S, the electron transfer step associated with the Fe-S movement was similar to that seen with the native enzyme (i.e., too fast to be time resolved) (Figure 3 and not shown**)**. Thus, all but T288S mutations affected QH_2 oxidation per se rather than the movement of the Fe-S subunit at the Q_o site. Only in the case of T288S was a slow cyt *c* rereduction phase seen in the presence of myxothiazol (Figure 3, panel F). However, in the absence of inhibitor this electron transfer

Table 2: Various Properties of the T288X Second-Site Suppressors

strains		Ps	assembly			electron transfer	
first mutation	second mutation	phenotype[a]	Fe-S subunit[b]	[2Fe2S] cluster[c]	EPR g_x[d]	rate (%)[e]	movement[f]
B:T288G	F:V44F	slow	35	65	1.789	20	fast
B:T288N	F:A46T	+	85	100	1.805	70	fast
B:T288N	F:V44F	+	45	35	nd[g]	nd	fast
B:T288S	F:V139A	+	115	80	1.807 and 1.772	25	slow
B:T288S	B:G182S	slow	30	35	1.800 and 1.768	11	fast
B:T288S	B:A185V	slow	130	100	1.803 and 1.781	15	fast
B:T288S	B:A185V + F:A46T	+	100	90	1.802 and 1.78	35	fast

[a] (+) or (slow) indicates the normal or slow photosynthetic growth in MPYE-enriched medium, and slow indicates that the Ps growth is at a rate slower than that of a wild-type strain. [b] Fe-S subunit refers to the stoichiometry of the Fe-S subunit to cyt c_1 or cyt *b* subunits as determined by scanning of the SDS−PAGE gels and immunoblots as described in ref *24* and is expressed as a percentage of the wild type. [c] [2Fe2S] cluster refers to the relative amounts of the [2Fe2S] cluster in the mutants in comparison with the wild type, as determined by the amplitude of their EPR g_y signal in the presence of the inhibitor stigmatellin and normalized for protein concentrations of chromatophore membranes. [d] Position of the EPR g_x signal in the absence of inhibitor and with the Q_{pool} oxidized. Note that for the T288S revertants two g_x signals were observed. [e] Electron transfer rate reflects single turnover bc_1 complex activity and corresponds to the average of QH_2 to cyt *c* and QH_2 to cyt *b* electron transfer rates. These rates expressed as a percentage of that of the wild-type enzyme (approximately 300 and 500 s^{-1} for cyt *c* rereduction and cyt *b* reduction kinetics, respectively) were not significantly different from each other and were determined as described in Materials and Methods. [f] Fast or slow movement is defined according to ref *23* and depends upon whether the initial phase corresponding to the electron transfer from the [2Fe2S] cluster to c_1 heme in the presence of myxothiazol is visible or not. [g] nd: not done.

reached only the level seen in the presence of myxothiazol, and no Q_o site turnover could be observed. We therefore concluded that in T288S both the QH_2 oxidation and the movement of the Fe-S subunit were perturbed.

Various Regions of the bc_1 Complex Interact Closely with the Fe-S Subunit during QH_2 Oxidation and Large-Scale Domain Movement. The role of the cyt *b ef* loop on Q_o site catalysis was further investigated by analyzing Ps^+ revertants of various T288X substitutions that were isolated on MPYE-enriched medium. Starting with T288D or T288G, or with T288S, the same site revertants T288V or T288I, respectively, were obtained. These revertants recovered a wild-type-like EPR signal (g_x around 1.8) (Table 1) and a moderate bc_1 complex activity (Figures 1 and 3 and not shown). Alternately, revertants containing secondary mutation(s) located elsewhere than position 288 of cyt *b* were also sought. In each case, spontaneous Ps^+ colonies were obtained, their plasmids extracted, and their *pet* operons cut into small fragments and exchanged with their counterparts on a plasmid carrying the parental T288X mutation. This approach enabled us to target directly the search for secondary mutation(s) to predefined regions of the bc_1 complex. Subsequent sequencing of the exchanged DNA fragments revealed three different groups of second-site revertants.

The first group of second-site mutations such as V44F and A46T were located on the hinge domain of the Fe-S subunit and obtained starting with the T288G and T288N substitutions. The properties of the corresponding double mutants are listed in Table 2, and their locations are depicted in Figure 4. In B:T288G + F:V44F and B:T288N + F:A46T the second mutation shifted upfield the g_x transition (e.g., from 1.77 to 1.789 for the former mutant) (Figure 1B) and improved the function of the bc_1 complex (Figure 3, panel L) but at the expense of the Fe-S subunit stability. Remarkably, the two second-site mutations F:V44F and F:A46T have already been encountered as suppressors of the F:L136G mutation located at the Fe-S subunit cluster domain (*45*) and characterized by Brasseur et al. (*46*). In particular, it has been found that these mutations increased the sensitivity of the Fe-S subunit hinge domain to proteolysis by an endogenous protease present in chromatophore membranes (*25* and not

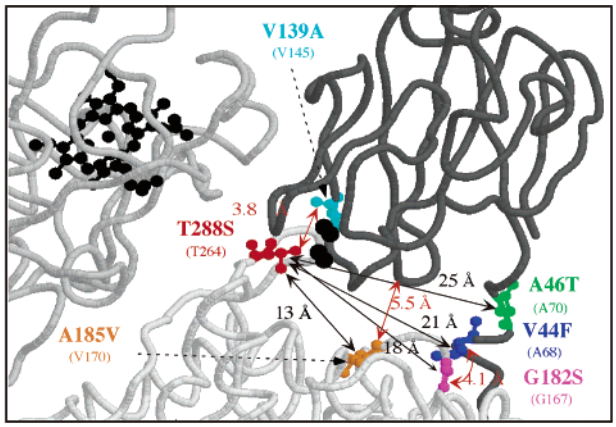

FIGURE 4: Locations of *R. capsulatus* T288X substitutions and their second-site suppressors. The figure is to visualize the positions of the different mutations described in this work using the coordinates of the bovine heart mitochondrial bc_1 complex with the Fe-S subunit in the intermediate position (*14*). Part of cyt c_1, cyt *b*, and the Fe-S subunits are shown in various shades of gray, and the cofactors (c_1 heme and the [2Fe2S] cluster) are in black. The amino acid residues occupying positions 167, 170, and 264 of cyt *b* and positions 68, 70, and 145 of the Fe-S subunit in bovine numbering (corresponding to *R. capsulatus* positions 182, 185, and 288 of cyt *b* and positions 44, 46, and 139 of the Fe-S subunit, respectively) are shown as ball-and-stick representation in magenta, orange, red, blue, green, and cyan. Distances between these various positions are indicated in angstroms.

shown). In addition, the F:A46T mutation has also been encountered as a suppressor of the B:T163F mutation that was located at the Q_oI domain of cyt *b* subunit and that destroyed the assembly of the bc_1 complex (*47*).

The second group of second-site mutations, like F:V139A that alleviated the defect of the T288S mutation, were found located on the Fe-S subunit cluster domain (Figure 4). EPR analyses of the double mutant T288S + F:V139A indicated that it exhibited multiple g_x signals with one around 1.8 and another around 1.77, suggesting the presence of two subpopulations that are in disequilibrium at 20 K (Figure 1 and Table 2). Nonetheless, in this mutant, electron transfer rates from QH_2 to cyt *c* were improved to about 25% of that of a wild-type strain, although the movement of the cluster

domain remained hindered as reflected by similar kinetics observed in the presence of myxothiazol (Figure 3, panel I).

The third group of second-site mutations, like G182S and A185V that alleviated the defect inflicted by T288S, were located on the *cd* loop of cyt *b* subunit (Figure 4). They exhibited poor bc_1 complex activity as well as slow Ps growth (Table 2 and Figure 3, panel J). Moreover, B:G182S, which was also encountered previously as a suppressor of the B:T163F mutant (*47*) like F:A46T, affected the assembly or stability of the Fe-S subunit. Finally, the slower Ps growth phenotype of the double mutant B:T288S + B:A185V allowed further isolation of better growing colonies that harbored a third mutation, F:A46T, located at the hinge region of the Fe-S subunit (Figure 3, panel K). It was noted that the mixed g_x signals of the [2Fe2S] cluster were present in all of the T288S suppressors (B:T288S + F:139A, BT288S + B:G182S, and B:T288S + B:A185V) (Table 2), suggesting that this feature was an intrinsic property of this substitution.

In summary, overall analyses of the second-site compensatory mutations of T288S revealed close protein−protein interactions between the hinge and the head domains of the Fe-S subunit and the *cd* and *ef* loops of the cyt *b* subunit of the bc_1 complex during Q_o site catalysis.

DISCUSSION

Intricacy of the Interactions between Cyt b and the Fe-S Subunit. Our earlier work has shown that mutations such as B:L286F located on the *ef* loop of cyt *b* could alleviate the movement hindrance implicated by the F:+1Ala mutation located at the hinge region of the Fe-S subunit of the bc_1 complex (*32*). In this study, we have probed the role of position 288, located two residues away but on the opposite face of this surface loop. Using the bacterial bc_1 complex, we first substituted position 288 with various amino acid residues and discovered that only a few hydrophobic side chains (Val, Ile, or Leu) could yield partly functional bc_1 complexes. Other substitutions exhibited assembly or stability defects, very low or no catalytic activity, and defective interactions between the [2Fe2S] cluster and the Q_o site occupants. Surprisingly, at this highly conserved position of cyt *b* even side chains such as Ser and Cys that are somehow similar to Thr were not readily tolerated, underlining the specific role that position 288 plays for Q_o site occupancy and catalysis. Moreover, the T288S substitution also interfered with the mobility of the Fe-S subunit cluster domain, pointing out protein−protein interactions between the *ef* loop of cyt *b* and the Fe-S subunit cluster domain during its movement.

Additionally, an absolute requirement of a functional bc_1 complex for Ps growth ability of *R. capsulatus* was exploited to obtain revertants that compensated the defects inflicted by the T288X substitutions. Among them, second-site suppressors located either at the hinge or the cluster domain of the Fe-S subunit or at the *cd* loop of cyt *b* were found. Interestingly, several of these secondary mutations, such as F:V44F, F:A46T, and B:G182S, had already been encountered previously as suppressors of defective Q_o site mutations located either at the cluster domain of the Fe-S protein (F:L136G) (*46*) or at the *cd* loop of cyt *b* (B:T163F) (*47*). Furthermore, several additional Q_o site suppressors, such as F:V139A located at the cluster domain of the Fe-S subunit and B:A185V on the *cd* loop of cyt *b*, were isolated for the first time during this work. Upon examination of the bc_1 complex structure one can envision that B:T288S suppressors located at the Fe-S subunit cluster domain (such as F:V139A) could be expected as this domain faces directly the *ef* loop of cyt *b* (Figure 4). However, as the cluster domain moves, protein−protein interactions that it entertains must remain complementary during its entire trajectory. Consequently, this suppressor does not appear to overcome steric hindrances during the movement, but rather it enables the cluster domain to reach a conformation appropriate for somewhat productive interactions with the Q_o site residents to restore a proper g_x signal and some catalytic activity. Similarly, B:T288S suppressors on the hinge region of the Fe-S subunit (such as F:V44F or F:A46T) could be expected because the converse situation, that is, mutations situated on the *ef* loop acting as suppressors of mutations located on the hinge region of the Fe-S subunit, had been encountered previously (*32*). On the other hand, suppressors on the cyt *b* *cd* loop (such as G182S and B:A185V) were less obvious even though this loop also comes very close to the Fe-S subunit. For example, B:A185 (Val170 in bovine numbering) is only 5.5 Å away from F:G93 of the Fe-S subunit cluster domain, and B:G182 is only 4 Å away from F:V44 of the hinge domain (Figure 4). Moreover, NEM labeling of a bc_1 complex carrying the B:A185C mutation in *Rhodobacter sphaeroides* had indicated that this position affects the interactions of the [2Fe2S] cluster with the Q_o site (*48*). Clearly, the effects of the T288S suppressors are indirect, yet they could change directly the conformation of the *cd* loop, which in turn by being close to the hinge and the cluster domains of the Fe-S protein interfere with its position and mobility at the Q_o site (*42*). Conceivably, as the trajectory of the Fe-S cluster domain is complex, composed of a rotation and a translation, even a small change can displace the rotation axis enough to induce significant remote interactions.

Multiple Functions of the ef Loop of Cyt b. Detailed examination of various T288X mutations indicated that the cyt *b* *ef* loop plays several roles in regard to Q_o site catalysis. First, as revealed by the T288K, T288R, and T288Y substitutions and also by L286F mutation (*32*), it affects the stability or assembly of the Fe-S subunit in the bc_1 complex. The basis of this effect is unclear, but it could be that in the absence of L286 or T288 the Fe-S subunit may not reach its native position at the surface of cyt *b*, and consequently its binding to the bc_1 complex could be weaker. Alternatively, in the T288X mutants the Fe-S subunit being in a more "released" position (i.e., structurally reminiscent of that observed when the Q_o site is occupied with myxothiazol) (*16*), the linker region of the Fe-S subunit may be more vulnerable to proteolytic cleavage by endogenous proteases (*25*). Another possibility is that if the Q_o site, and in particular the [2Fe2S] cluster, is more solvent exposed as suggested by its broader g_x transition, then its increased lability may render the apoprotein less stable.

Second, most of the T288X mutations are defective to varying degrees for QH_2 oxidation, which indicates that a major role of position 288 on the *ef* loop is on Q_o site catalysis. In most mutants, the interactions of the [2Fe2S]

cluster with Q were perturbed as revealed by shifted EPR g_x signals. In their revertants a partial restoration of the native $g_x = 1.8$ transition was observed concomitantly with a gain of activity. The basis of the mixed EPR signal observed in the T288S revertants is unclear at the moment, but further studies might indicate whether this reflects two distinct populations of enzymes with their Fe-S subunits in two different positions not in equilibrium at cryogenic temperature or, simply, partial Q depletion at the Q_o site in response to the *ef* loop mutations. Moreover, the lower E_m values of the Fe-S subunits in these mutants suggest that their cluster domains are no longer in their native position. The overall data, in particular the lower E_m values, suggested that in the T288N and T288S mutants the [2Fe2S] clusters might be located in an environment more hydrophilic as compared with a native bc_1 complex, and the head domain of their Fe-S subunits was in a more released position, as discussed previously (*42*). As also shown in ref *42*, the E_m of the [2Fe2S] cluster increases when it reaches in the Q_o site a subdomain that is appropriate for catalysis. Thus, a critical role for the *ef* loop would be to facilitate this step by promoting favorable interactions, such as providing additional hydrogen bonds to the Fe-S subunit. The QH_2 oxidation defects encountered in the T288X mutants are consistent with various mechanisms proposed previously (*7*−*10*), including the concerted mechanism proposed by Snyder et al. (*11*) which stipulates a simultaneous interaction of UQH_2 with His161 on the Fe-S subunit and Glu272 on cyt *b* (Glu295 in *R. capsulatus* numbering). Conceivably, changing the conformation of the *ef* loop by T288 mutations could easily result in altered interactions with Glu295, leading to perturbed QH_2 oxidation.

Remarkably, the T288S substitution and its revertants reveal that in these mutants, in addition to the Q_o site catalysis defect, the movement of the Fe-S subunit cluster domain is also hindered. This situation is reminiscent of that previously seen with the +1Ala hinge mutant and its B:L286F revertant (*23*, *32*), again indicating that the *ef* loop of cyt *b* can also interfere with the mobility of the Fe-S subunit during its large-scale domain movement. Indeed, steered molecular dynamics simulations of the Fe-S subunit movement performed by Izrael et al. (*31*) are consistent with this suggestion as they indicate that the *ef* loop domain (residues 263−268 corresponding to residues 286−291 in *R. capsulatus* numbering) of cyt *b* may be displaced by about 2 Å when the Fe-S subunit moves out of the Q_o site, with several hydrogen bonds forming between this loop and the Fe-S cluster domain.

In summary, this work revealed several important roles played by surface loops *cd* and *ef* of cyt *b*, which form a tight gasket at the Q_o site to prevent excessive solvent accessibility, to hold the Fe-S subunit cluster domain in a position appropriate for productive interactions between the [2Fe2S] cluster and Q_o site occupants, and to ensure stability of the Fe-S subunit in the bc_1 complex. Apparently, this seal is not too tight in order to allow the Fe-S subunit cluster domain to reach its proper position at the Q_o site and not to hinder its large-scale movement to donate electrons to the c_1 heme. Various suppressors of T288 indicated that multiple regions of cyt *b* contribute to finely adjust the Fe-S subunit/cyt *b* interface at the Q_o site. Further mapping of additional interactions between these subunits may extend the network of interactions in terms of stability, catalysis, [2Fe2S] cluster domain position, and movement of the Fe-S subunit at the Q_o site and better elucidate the various steps of QH_2 oxidation catalyzed by the bc_1 complex.

REFERENCES

1. Gennis, R. B., Barquera, B., Hacker, B., Van, D. S. R., Arnaud, S., Crofts, A. R., Davidson, E., Gray, K. A., and Daldal, F. (1993) *J. Bioenerg. Biomembr. 25*, 195−209.
2. Gray, K. A., and Daldal, F. (1995) in *Anoxygenic Photosynthetic Bacteria* (Blankenship, R. E., Madigan, M. T., and Bauer, C., Eds.) pp 747−774, Kluwer Academic Publishers, Dordrecht, The Netherlands.
3. Yu, C.-A. (1999) *J. Bioenerg. Biomembr. 31*(3) (special issue on cytochrome bc_1).
4. Cramer, W., Soriano, G., Ponomarev, M., Huang, D., Zhang, H., Martinez, S., and Smith, J. (1996) *Annu. Rev. Plant Physiol. 47*, 477−508.
5. Crofts, A. R., Meinhardt, S. W., Jones, K. R., and Snozzi, M. (1983) *Biochim. Biophys. Acta 723*, 202−218.
6. Dutton, P. L.,Ohnishi, T., Darrouzet, E., Leonard, M. A., Sharp, R. E., Gibney, B. R., Daldal, F., and Moser, C. C. (2000) in *Coenzyme Q: Molecular Mechanisms in Health and Disease* (Kagan, V. E., and Quinn, P. J., Eds.) pp 65−82, CRC Press, Boca Raton, FL.
7. Ding, H., Moser, C. C., Robertson, D., Tokito, M., Daldal, F., and Dutton, P. L. (1995) *Biochemistry 34*, 15979−15996.
8. Brandt, U. (1996) *FEBS Lett. 387*, 1−6.
9. Crofts, A. R., Hong, S., Ugulava, N., Barquera, B., Gennis, R., Guergova-Kuras, M., and Berry, E. A. (1999) *Proc. Natl. Acad. Sci. U.S.A. 96*, 10021−10026.
10. Link, T. (1997) *FEBS Lett. 412*, 257−264.
11. Snyder, C. H., Gutierrez-Cirlos, E. B., and Trumpower, B. L (2000) *J. Biol. Chem. 275*, 13535−13541.
12. Xia, D., Yu, C.-A., Kim, H., Xia, J. Z., Kachurin, A. M., Zhang, L., Yu, L., and Deisenhofer, J. (1997) *Science 277*, 60−66.
13. Zhang, Z., Huang, L., Shulmeister, V. M., Chi, Y.-I., Kim, K. K., Hung, L.-W., Crofts, A. R., Berry, E. A., and Kim, S.-H. (1998) *Nature 392*, 677−684.
14. Iwata, S., Lee, J. W., Okada, K., Lee, J. K., Iwata, M., Rasmussen, B., Link, T. A., Ramaswamy, S., and Jap, B. K. (1998) *Science 281*, 64−71.
15. Hunte, C., Koepke, J., Lange, C., Rossmanith, T., and Michel, H. (2000) *Structure 8*, 669−684.
16. Kim, H., Xia, D., Yu, C.-A., Xia, J.-Z., Kachurin, A. M., Zhang, L., Yu, L., and Deisenhofer, J. (1998) *Proc. Natl. Acad. Sci. U.S.A. 95*, 8026−8033.
17. Brugna, M., Rodgers, S., Schricker, A., Montoya, G., Kazmeier, M., Nitschke, W., and Sinning, I. (2000) *Proc. Natl. Acad. Sci. U.S.A. 97*, 2069−2074.
18. Obungu, V. H., Wang, Y., Amyot, S. M., Gocke, C. B., and Beattie, D. S. (2000) *Biochim. Biophys. Acta 1457*, 36−44.
19. Nett, J. H., Hunte, C., and Trumpower, B. L. (2000) *Eur. J. Biochem. 267*, 5777−5782.
20. Tian, H., Yu, L., Mather, M. W., and Yu, C.-A. (1998) *J. Biol. Chem. 273*, 27953−27959.
21. Tian, H., White, S., Yu, L., and Yu, C.-A. (1999) *J. Biol. Chem. 274*, 7146−7152.
22. Xiao, K., Yu, L., and Yu, C.-A. (2000). *J. Biol. Chem. 275*, 38597−38604.
23. Darrouzet, E., Valkova-Valchanova, M., Moser, C. C., Dutton, P. L., and Daldal, F. (2000) *Proc. Natl. Acad. Sci. U.S.A. 97*, 4567−4572.
24. Darrouzet, E., Valkova-Valchanova, M., and Daldal, F. (2000) *Biochemistry 39*, 15475−15483.
25. Valkova-Valchanova, M., Darrouzet, E., Moomaw, C. R., Slaughter, C. A., and Daldal, F. (2000) *Biochemistry 39*, 15484−15492.
26. Darrouzet, E., Moser, C. C., Dutton, P. L., and Daldal, F. (2001) *Trends Biochem. Sci. 26*, 445−451.
27. Breyton, C. (2000) *J. Biol. Chem. 275*, 13195−13201.
28. Rao, S. B. K., Tyryshkin, A. M., Roberts, A. G., Bowman, M. K., and Kramer, D. M. (2000) *Biochemistry 39*, 3285−3296.
29. Roberts, A. G., Bowman, M. K., and Kramer, D. M. (2002) *Biochemistry 41*, 4070−4079.
30. Gray, K., Dutton, P. L., and Daldal, F. (1994) *Biochemistry 33*, 723−733.

31. Izrailev, S., Crofts, A. R., Berry, E. A., and Schulten, K. (1999) *Biophys. J. 77*, 1753−1768.
32. Darrouzet, E., and Daldal, F. (2002) *J. Biol. Chem. 277*, 3471−3476.
33. Atta-Asafo-Adjei, E., and Daldal, F. (1991) *Proc. Natl. Acad. Sci. U.S.A. 88*, 492−496.
34. Lowry, O., and Rosebrough, N. (1951) *J. Biol. Chem. 193*, 265−275.
35. Dutton, P. L. (1978) *Methods Enzymol. 54*, 411−435.
36. Gray, K., Dutton, P. L., and Daldal, F. (1994) *Biochemistry 33*, 723−733.
37. Ding, H., Robertson, D. E., Daldal, F., and Dutton, P. L. (1992) *Biochemistry 31*, 3144−3158.
38. von Jagow, G., and Ohnishi, T. (1985) *FEBS Lett. 185*, 311−315.
39. Sharp, R. E., Palmitessa, A., Gibney, B. R., Moser, C. C., Daldal, F., and Dutton, P. L. (1998) *FEBS Lett. 431*, 423−426.
40. Sharp, R. E., Gibney, B. R., Palmitessa, A., White, J. L., Moser, C. C., Daldal, F., and Dutton, P. L. (1999) *Biochemistry 38*, 14973−14980.
41. Roberts, A. G., and Kramer, D. M. (2001) *Biochemistry 40*, 13407−13412.
42. Darrouzet, E., Valkova-Valchanova, M., and Daldal, F. (2002) *J. Biol. Chem 277*, 3464−3470.
43. Crofts, A. R., Hong, S., Zhang, Z., and Berry, E. A. (1999) *Biochemistry 38*, 15827−15839.
44. Saribas, A. S., Ding, H., Dutton, P. L., and Daldal, F. (1995) *Biochemistry 34*, 16004−16012.
45. Liebl, U., Sled, V., Brasseur, G., Ohnishi, T., and Daldal, F. (1997) *Biochemistry 36*, 11675−11684.
46. Brasseur, G., Sled, V., Liebl, U., Ohnishi, T., and Daldal, F. (1997) *Biochemistry 36*, 11685−11696.
47. Saribas, A. S., Valkova-Valchanova, M., Tokito, M. K., Zhang, Z., Berry, E. A., and Daldal, F. (1998) *Biochemistry 37*, 8105−8114.
48. Tian, H., Yu, L., Mather, M. W., and Yu, C.-A. (1997) *J. Biol. Chem. 272*, 23722−23728.

BI026656H